Available online at www.sciencedirect.com

Journal of Applied Research and Technology

Journal of Applied Research and Technology 15 (2017) 378–385

www.jart.ccadet.unam.mx

Original

Application of nanoscale ZnS/TiO_2 composite for optimized photocatalytic decolorization of a textile dye

Sajad Talebi, Naz Chaibakhsh *, Zeinab Moradi-Shoeili

Department of Chemistry, Faculty of Sciences, University of Guilan, Rasht 4193833697, Iran

Received 19 October 2016; accepted 15 March 2017
Available online 26 August 2017

Abstract

The synthesis of ZnS/TiO_2 nanocomposite was successfully performed by a chemical deposition method. The structure and morphology of the prepared catalyst were characterized by X-ray diffraction (XRD), scanning electron microscopy (SEM), energy dispersive X-ray (EDX), and FT-IR spectroscopy. The activity of the photocatalyst was evaluated for the removal of Acid Blue 113 (AB113) dye in aqueous solution under UV-A radiation. Response surface methodology (RSM) based on the central composite rotatable design (CCRD) was applied to study and optimize the photodegradation process. The effects of three experimental parameters including pH, irradiation time, and the catalyst dose on the AB113 removal were studied. A high dye removal (99.0%) was obtained by using minimum amount of the catalyst (37 mg) at the optimal conditions of 27.32 min and pH 6.18. Compared with pure nano-sized TiO_2 and ZnS, the synthesized nanocomposite exhibited a higher photocatalytic activity. The kinetics of AB113 adsorption on the surface of ZnS/TiO_2 nanocomposite could be described by the pseudo second order and parabolic-diffusion models.

Keywords: Acid Blue 113; Central composite design; Dye removal; Photocatalysis; ZnS/TiO_2 nanocomposite

1. Introduction

Wastewaters generated from dye-manufacturing and dye-consuming industries have always been an issue of environmental concern. The presence of dyes in effluents leads to reduction in sunlight penetration and photosynthetic activities of aquatic ecosystem, and increase in biochemical oxygen demand (Singh, Mohan, Sinha, Tondon, & Gosh, 2003). Dyes are generally recalcitrant organic compounds that cannot be easily removed by biological treatment systems (Gosavi & Sharma, 2014). However, the application of non-biological procedures, such as photocatalytic advanced oxidation process, could result in satisfactory elimination (Tseng et al., 2012).

Photocatalysis of dyes involves the formation of highly reactive oxygen species (ROS) like hydroxyl and superoxide radicals to react with dyes and degrade them in the presence of a semiconductor and visible or ultraviolet (UV) light (Muhd Julkapli, Bagheri, & Bee Abd Hamid, 2014).

Among the various semiconductor oxides, TiO_2 and ZnS have been widely used for degradation of organic pollutant molecules due to their photoactivity, stability, and non-toxicity (Dhatshanamurthi, Subash, Krishnakumar, & Shanthi, 2014; Pouretedal & Sohrabi, 2016). However, compared with the solitary TiO_2 or ZnS, the photocatalytic activity of ZnS/TiO_2 composite can be improved greatly due to the quantum confinement effects (Wang & Zhang, 2014).

In this study, the coupled semiconductors, ZnS/TiO_2, with nanometer size, were synthesized by a chemical deposition method. The prepared nanocomposite was used for photocatalytic degradation of Acid Blue 113 (AB113) dye. AB113 is a popular industrial diazo dye, extensively used for dyeing wool, leather, silk, nylon and polyester fiber (De Moura, Quiroz, Da Silva, Salazar, & Martínez-Huitle, 2016; Nachiyar et al., 2012). So far, there is no report on the photodegradation of AB113 by nanoscale ZnS/TiO_2 composite.

To increase and optimize the dye degradation efficiency of the prepared photocatalyst, response surface methodology (RSM) with central composite rotatable design (CCRD) was used. RSM

* Corresponding author.
E-mail address: nchaibakhsh@guilan.ac.ir (N. Chaibakhsh).

Peer Review under the responsibility of Universidad Nacional Autónoma de México.

http://dx.doi.org/10.1016/j.jart.2017.03.007

is a statistical technique used for empirical model building and analyzing the relationships between a number of experimental input parameters and a response. Compared to one-variable-at-a-time (OVAT) method, optimization by RSM requires less time and experiments and is more accurate (Wani, Ahmad, Zargar, Khalil, & Darwish, 2012). RSM has been successfully employed for optimization of photodegradation of various dyes (Dostanić et al., 2013; Vaez, Zarringhalam Moghaddam, & Alijani, 2012). However, the application of RSM in the photocatalytic degradation of AB113 has not been reported yet.

The aim of this study was to investigate the possibility of photocatalytic degradation of AB113 dye in the presence of synthesized ZnS/TiO_2 nanocomposite under UV irradiation. The dye degradation efficiency of ZnS/TiO_2 was compared with intrinsic nano-sized anatase TiO_2 and synthesized ZnS nanoparticles. RSM and CCRD were employed to optimize and analyze the effects of three operational parameters including pH, irradiation time, and the catalyst dose on the dye photodegradation efficiency.

2. Materials and methods

2.1. Materials and apparatus

All materials were obtained from commercial sources and used as received without further purification. Nano-sized anatase TiO_2 (<25 nm) powder with purity of >99% was purchased from Sigma–Aldrich. X-Ray Diffraction pattern (XRD) of the synthesized nanoparticle powders were recorded in 2θ range from 10° to 80° by using a high resolution X-Ray Diffractometer (Philips PW 1830 diffractometer) with Cu-Kα radiation ($\lambda = 1.54$ Å). FT-IR spectra of the samples in the form of KBr pellets were recorded using an Alpha-Bruker FT-IR spectrophotometer. The scanning electron (SEM) images were taken by a LEO 1430 VP (Carl Zeiss, Germany) scanning electron microscope. The elemental analysis was recorded with an energy dispersive X-ray (EDX) analyzer, MIRA3 FEG-SEM series.

2.2. Synthesis and characterization of ZnS nanoparticles

The ZnS nanoparticles were prepared following the previously published procedure (Bai et al., 2014). In a typical synthesis procedure, 0.38 g of thioacetamide was added to a solution of 1.5 g of zinc nitrate hexahydrate ($Zn(NO_3)_2{\cdot}6H_2O$) in 37.5 mL ethanol and the mixed solution was stirred at room temperature for 30 min. The mixture was transferred into a Teflon-lined autoclave of 100 mL capacity and heated at 120 °C for 5 h. The resulting deposition was recovered by centrifugation, washed with distilled water and ethanol for several times in order to remove residual ions. The resultant product was dried at 60 °C for 10 h.

2.3. Synthesis of ZnS/TiO_2 hybrid photocatalyst

The nanocomposite particles of ZnS/TiO_2 were prepared according to the methods described previously (Franco et al., 2009). The first step involves the synthesis of zinc diethyldithiocarbamate by addition of ethylenediamine (20 mmol, 1.33 mL) and CS_2 (13.5 mmol, 0.8 mL) to a suspension of $ZnCl_2{\cdot}4H_2O$ (6.5 mmol, 1.36 g) in 50 mL water. The white solid was obtained after stirring the reaction mixture for 2 h. In the next step, ethylenediamine (2.5 mL) was added dropwise to an acetone solution (47.5 mL) of zinc dithiocarbamate complex and 0.125 g of TiO_2 naoparticles. The suspension was refluxed for 4 h. The white solid product was collected by centrifugation, washed with acetone and dried at room temperature.

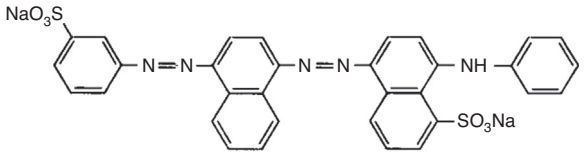

Fig. 1. The chemical structure of AB113 dye.

2.4. Photocatalysis experiments

The photochemical reactor was a beaker containing suspension of the photocatalyst and AB113 dye solution of 25 mg/L placed in a continuously ventilated chamber. Irradiation in the UV-A region (400–315 nm) was provided by a 400 W Kr UV lamp, Osram. The distance between the UV source and the reactor was 30 cm. The suspension was magnetically stirred during irradiation. Before irradiation, the sample was stirred for 5 min to reach an adsorption–desorption equilibrium between the dye molecules and the catalyst surface (Zanjanchi, Golmojdeh, & Arvand, 2009).

2.5. Dye removal assay

Acid Blue 113 is a diazo group-containing acid dye (Fig. 1). It is dark blue/black powder, which is soluble in water. The dye was supplied by a textile manufacturing company. A dye solution of 25 mg/L was prepared by dissolving AB113 in distilled water. The pH of the solution was adjusted in the range of 3.0–8.0 by addition of diluted HCl or NaOH using a pH meter (AZ Instrument, model 86502). Two-hundred milliliter of the solution was put into 250 mL-flask, and various doses of catalyst (10–60 mg) were added. After irradiation for a certain period of time (2–30 min), the photocatalyst particles was removed by centrifugation. Color removal was measured using a spectrophotometer (Model UV 2100, Shimadzu Co., Kyoto, Japan) at the maximum absorbency wavelength of 518 nm. The AB113 removal percentage was calculated using the following equation:

$$\text{Dye removal} \quad (\%) = 100\frac{[A_0 - A]}{A_0} \tag{1}$$

where A is the average of absorbance values at 518 nm after the treatment process, and A_0 the value before treatment.

Table 1
Composition of various experiments of the CCRD, and AB113 photodegradation percentages.

Exp.No.	Variable			AB 113 removal (%)
	Catalyst dose (mg)	pH	Time (min)	
1	35.00	5.50	16.00	82.59
2	49.87	6.99	7.68	59.07
3	49.87	4.01	7.68	23.39
4	20.13	4.01	24.32	57.73
5	49.87	4.01	24.32	82.76
6	35.00	3.00	16.00	36.67
7	35.00	5.50	30.00	94.12
8	20.13	6.99	24.32	70.84
9	10.00	5.50	16.00	32.46
10	20.13	4.01	7.68	29.48
11	35.00	8.00	16.00	78.25
12	20.13	6.99	7.68	57.09
13	35.00	5.50	16.00	80.00
14	60.00	5.50	16.00	54.34
15	35.00	5.50	2.00	22.24
16	49.87	6.99	24.32	99.20
17	35.00	5.50	16.00	85.21

2.6. Statistical analysis and optimization

A three-variable, five-level CCRD was employed for the design of experiments. The variables and their ranges selected for the photodegradation of AB113 by ZnS/TiO_2 were catalyst dose (10–60 mg), pH (3–8), and reaction time (2–30 min). The dye removal percentage was analyzed as the response. The employed design is presented in Table 1. Same experimental designs were used for the optimization of photodegradation of AB113 by nano-sized ZnS and TiO_2.

For RSM analysis, the levels of the factors were coded using the following equation:

$$\alpha = \frac{x_i - x_0}{\Delta x} \tag{2}$$

where α is the coded value of the variable; x_i is its real value; x_0 is its real value at the center point; and Δx is the step change in the variable.

After testing various models, a quadratic polynomial equation (Eq. (3)) was found to be suitable for studying the effects of the variables on the dye degradation:

$$y = \beta_0 + \sum_{i=1}^{k}\beta_i x_i + \sum_{i=1}^{k}\beta_{ii}x_i^2 + \left(\sum_{i=1}^{k-1}\sum_{j=i+1}^{k}\beta_{ij}x_i x_j\right)_{i<j} \tag{3}$$

where y is the response; x_i and x_j are the independent variables; β_0 is the constant coefficient; and β_i, β_{ii} and β_{ij} are the interaction coefficients.

An analysis of variance (ANOVA) was used to determine the adequacy of the generated model for describing the experimental data.

The Design Expert version 6.0.6 software (Stat-Ease, USA) was used for statistical analysis. Optimization was performed using a desirability function given in Eq. (4).

$$D = (d_1 \times d_2 \times \cdots d_n)^{1/n} = \left(\prod_{i=1}^{n} d_i\right)^{1/n} \tag{4}$$

where n is the number of responses in the measure and d_i is the desirable ranges for each response.

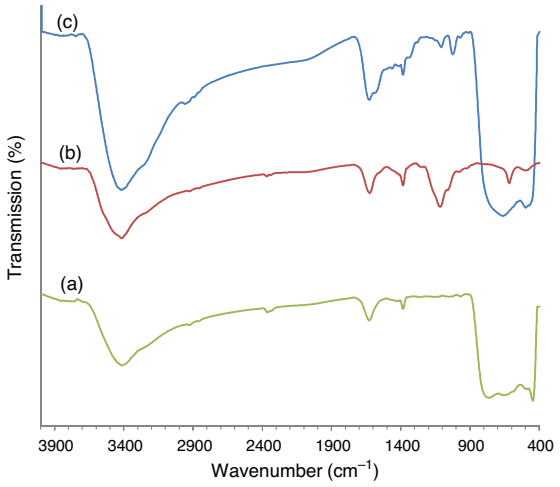

Fig. 2. FT-IR spectra of (a) TiO_2, (b) ZnS, and (c) ZnS/TiO_2 nanocomposite.

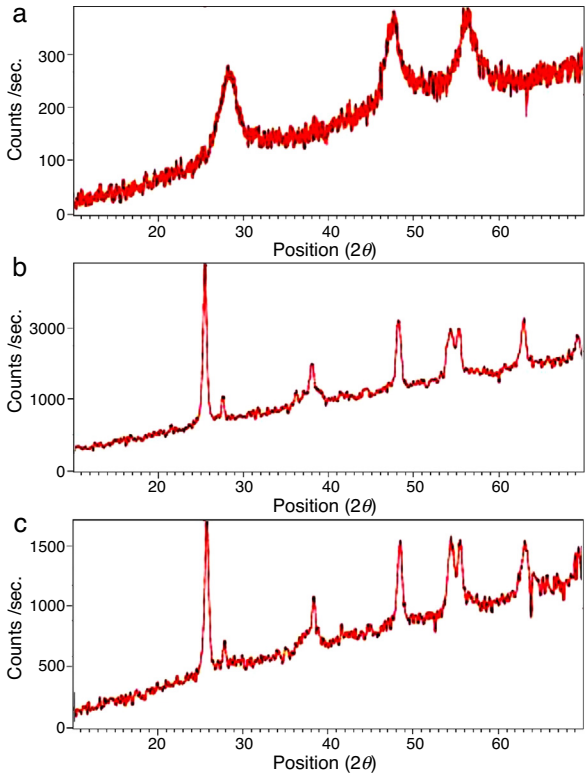

Fig. 3. The XRD patterns of (a) ZnS, (b) TiO_2, and (c) ZnS/TiO_2 samples.

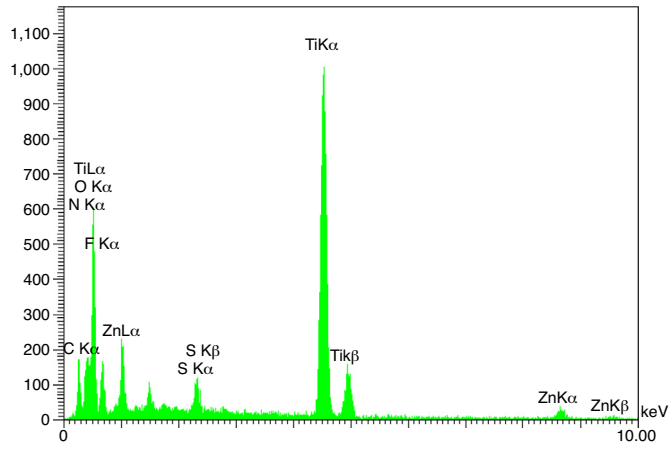

Fig. 4. EDX spectra of ZnS/TiO_2 powder sample.

2.7. Photodegradation kinetic models

In this study, six types of kinetic models were used as the decay models to analyze the kinetic data of the photodegradation of AB113 on ZnS/TiO_2 (Mukhlish, Najnin, Rahman, & Uddin, 2013; Sarici-Ozdemir, 2012). The models used include first-order (Eq. (5)), second order (Eq. (6)), pseudo first order (Eq. (7)), pseudo second order (Eq. (8)), modified Freundlich (Eq. (9)), and parabolic-diffusion (Eq. (10)) models.

$$\ln\left(\frac{C}{C_0}\right) = -kt \tag{5}$$

$$\frac{1}{C} - \frac{1}{C_0} = kt \tag{6}$$

$$\ln(C - C_0) = \ln C - kt \tag{7}$$

$$\frac{t}{C} = \frac{t}{C_0} - \frac{1}{kC^2} \tag{8}$$

$$\frac{C_0 - C_t}{C_0} = kt^b \tag{9}$$

$$\frac{(1 - C_t/C_0)}{t} = kt^{-1/2} + \alpha \tag{10}$$

3. Results and discussion

3.1. Catalyst preparation and characterization

The ZnS coupled TiO_2 nanocomposite was prepared using a chemical deposition method via the reaction of the zinc dithiocarbamate complex with ethylenediamine in the presence of TiO_2 nanoparticles. The FT-IR spectra of the synthesized material has been shown in Figure 2. The broad band centered at 500–600 cm^{-1} assigned to the vibration of the Ti–O bonds (Beranek & Kisch, 2008). The peak at around 1100 cm^{-1} is the characteristic ZnS vibration peak (Tian et al., 2016) that is absent from the pure TiO_2. This confirms the presence of ZnS in ZnS/TiO_2 nanoparticles. Strong bands at 1615–1635 cm^{-1} and the broad peaks appearing at 3100–3600 cm^{-1} are due to OH group of water molecules adsorbed to the surface of ZnS/TiO_2 product.

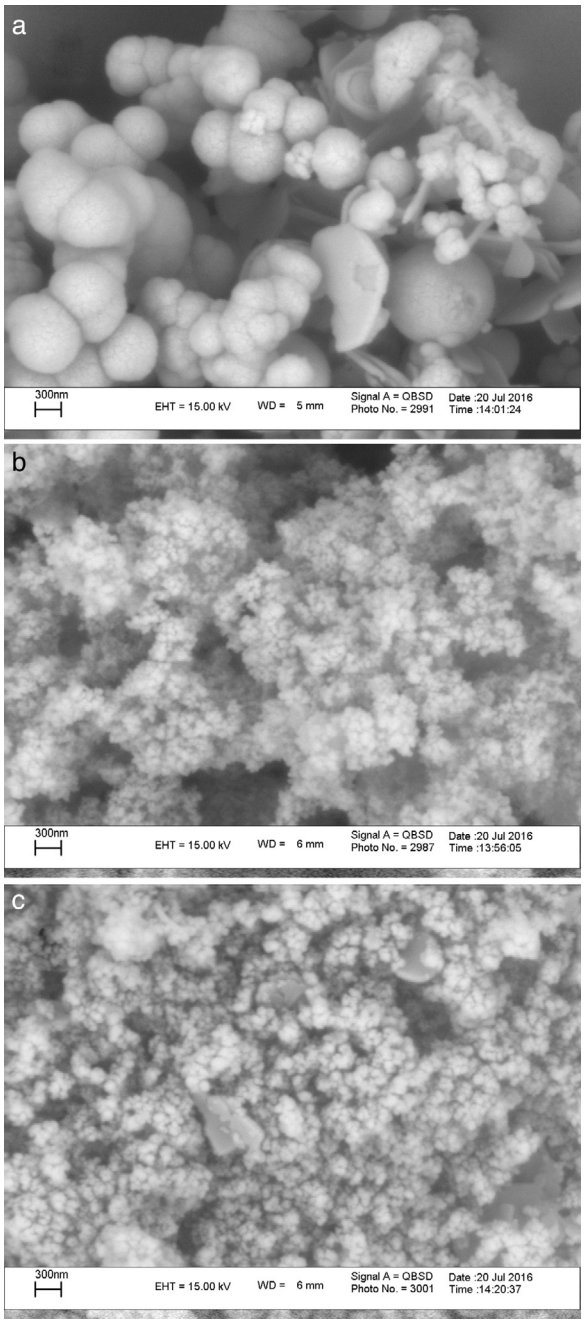

Fig. 5. SEM images for (a) ZnS, (b) TiO_2, and (c) ZnS/TiO_2 heterostructures nanocomposites.

The XRD patterns of the obtained ZnS/TiO_2 powder and parallel ZnS and TiO_2 samples are depicted in Figure 3. The XRD patterns of the pure ZnS sample (Fig. 3a) showed the typical reflection plans (111), (220), and (311) that can be indexed to the cubic phase of ZnS (Roychowdhury, Pati, Kumar, & Das, 2014). It is clear that the intensity of the peaks belonging to the ZnS nanoparticles in the diffraction pattern of ZnS/TiO_2 were lower than pure ZnS nanoparticles. Therefore, the characterization by X-ray diffraction patterns did not demonstrate relevant peaks of ZnS after the deposition on the surface of

TiO_2 nanoparticles (Fig. 3c). Broadening of the corresponding XRD peaks of ZnS in ZnS/TiO_2 sample can be attributed to the poor crystallinity and the small quantity of ZnS existing in the sample as well as the high crystallinity and small size of the TiO_2 (Senapati, Borgohain, & Phukan, 2012). However, the presence of ZnS, in ZnS/TiO_2 hybrid photocatalyst, was recognized by energy dispersive X-Ray (EDX) analysis. The elemental composition and distribution on the surface of the ZnS/TiO_2 nanoparticles was studied by EDX. The results shown in Figure 4 clearly demonstrated the presence of Ti, O, Zn and S in the nanocomposite which further confirms the identification of the ZnS/TiO_2 nanocomposites. The typical morphology and size of the obtained ZnS/TiO_2 nanoparticles were also determined by the scanning electron microscope (SEM). The results are presented in Figure 5. The morphological differences between TiO_2, ZnS and the ZnS/TiO_2 heterostructure are clearly observed using corresponding SEM images. It can be found that the flower like zinc sulfide particles are completely deposited on TiO_2 nanoparticles (Fig. 5c). The morphology is similar to that reported previously (Nageri, Kalarivalappil, Vijayan, & Kumar, 2016).

3.2. Model fitting and statistical analysis

Fitting of the coded experimental data to the quadratic multiple regression model showed that AB113 photodegradation on ZnS/TiO_2 could be described by the following equation:

$$\text{AB113 removal } (\%) = +82.04 + 6.30\,A + 11.92\,B + 19.21\,C - 11.92\,A^2 - 6.95\,B^2 - 6.70\,C^2 + 1.42\,AB + 7.19\,AC - 4.22\,BC$$

where A is photocatalyst dose (mg), B pH, and C irradiation time (min).

The ANOVA for the model is presented in Table 2. According to the results, all selected parameters have significant effects on the dye removal. The *F*-value of the model (25.18) with a *p*-value less than 0.05 (0.0002) implies that the model is significant at the 95% confidence level. The model also showed no lack of fit (*F*-value = 8.63). A high coefficient of determination ($R^2 = 0.97$) indicates that the generated model fits the data well. Therefore, the model can be used satisfactorily for analysis and optimization of the process (Myers, Montgomery, & Anderson-Cook, 2016).

3.3. Effect of parameters

Figure 6a, presents the response surface plot showing the effect of catalyst dose, pH, and their interactions on the AB113 removal at 16.0 min (the center point of the design). It was observed that the percentage of dye removal increased with increasing catalyst level up to 39.5 mg. After that, the dye degradation decreased. The increase in the amount of catalyst increases the number of active sites on the ZnS/TiO_2 surface that in turn increases the generation of ROS and hence the dye degradation. Above a certain catalyst amount (the saturation level), the number of available dye molecules is not sufficient to fill the active sites of the catalyst. An over optimum amount of photocatalyst lead to aggregation of the particles and increase in light scattering by the catalyst particles (Chaibakhsh, Ahmadi, & Zanjanchi, 2016; Giwa, Nkeonye, Bello, & Kolawole, 2012).

In a heterogeneous photocatalytic process, pH is an important parameter that affects the dye degradation mechanism (Jantawasu, Sreethawong, & Chavadej, 2009). According to Figure 6a, maximum dye removal was observed at pH 6.82. At low pH values, the formation of hydroxyl radicals will be suppressed due to an excessive concentration of H^+ and a low concentration of OH^- (Xue et al., 2015). After the optimum pH value, the degradation of AB113 started to decrease gradually due to repulsion between the negatively charged surface of the photocatalyst and hydroxide ions. In addition, at higher pH values, the oxidizing radicals are rapidly scavenged and cannot react with the dye molecules (Pare, Swami, More, Qureshi, & Thapak, 2011).

Figure 6b shows the effect of varying catalyst dose and UV-light irradiation time on the degradation of AB113 at pH = 5.5. By prolonging the time up to 30 min, the dye degradation increased. With increasing the radiation time, the number of absorbed photons on the catalyst surface becomes greater which promotes the photocatalytic process (Aisien & Blessing, 2013). Again, it can be seen that by increasing the catalyst up to an

Table 2
ANOVA for the model used for the analysis of AB113 degradation.

Source	Sum of squares	Degree of freedom	Mean square	*F*-value	*p*-Value
Model	9917.69	9	1101.97	25.18	0.0002
A, catalyst dose	542.54	1	542.54	12.40	0.0097
B, pH	1939.96	1	1939.96	44.33	0.0003
C, time	5041.21	1	5041.21	115.19	<0.0001
A^2	1602.33	1	1602.33	36.61	0.0005
B^2	544.70	1	544.70	12.45	0.0096
C^2	505.53	1	505.53	11.55	0.0115
AB	16.25	1	16.25	0.37	0.5616
AC	413.28	1	413.28	9.44	0.0180
BC	142.30	1	142.30	3.25	0.1143
Residual	306.34	7	43.76		
Lack of fit	292.77	5	58.55	8.63	0.1071
Pure error	13.57	2	6.79		
Corrected total	10,224.02	16			

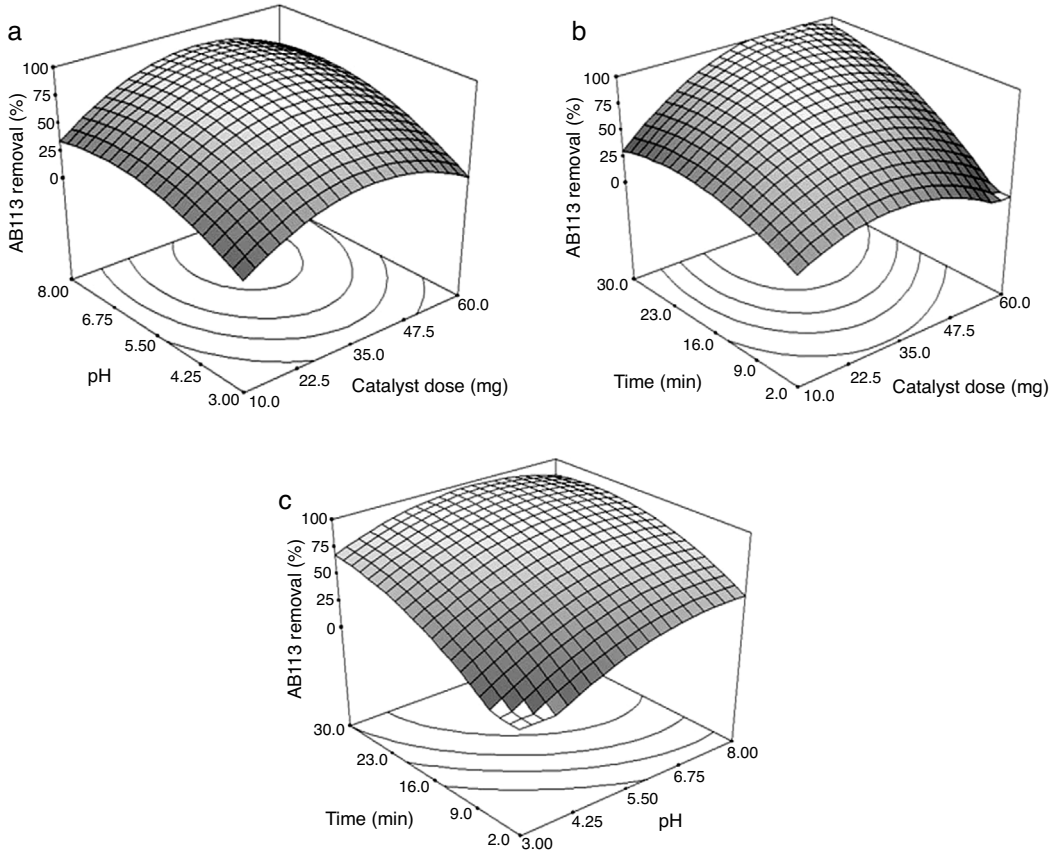

Fig. 6. Response surface plots showing the interaction between two parameters, pH and catalyst dose (a), irradiation time and catalyst dose (b), and irradiation time and pH (c) on the AB113 removal percentage.

optimum amount, the dye degradation increased. After that, a decrease in the removal percentage was observed.

Figure 6c depicts the response surface plot as a function of pH versus irradiation time using 35 mg of the catalyst. Maximum dye degradation percentage was observed at pH = 6.23 and 27 min. At lower pH, the effect of time was more significant. By increasing the time from 2 to 30 min at pH = 3, the percentage of phodegradation increased by around 70%. The results show that the optimum pH is in the range of 6.0–7.0. This pH range is within the limits of effluent discharge standards, therefore there would be no need for the adjustment of pH after the photodegradation process.

3.4. Optimum conditions

By using the optimization function of the software, RSM can predict the optimum combination of parameters to obtain the highest percentage of the dye degradation. Maximum dye removal (99.2%) by ZnS/TiO_2 nanocomposite was predicted under treatment conditions of 37 mg catalyst dose, pH 6.18, and 27.32 min. The actual experimental value obtained was 99.0%.

Optimization of the photodegradation of AB113 by pure nano-sized TiO_2 and ZnS was also performed by RSM. Maximum dye removal by TiO_2 was found to be 95.3% at 29.78 min, pH 6.56 and catalyst dose of 42 mg. Using the optimum condition found for the ZnS/TiO_2 nanocomposite, 89.5% dye removal was obtained for TiO_2. The results show that by using ZnS/TiO_2, a higher percentage of dye removal can be obtained using a lower amount of catalyst. On the other hand, using ZnS as the photocatalyst resulted in 17.3% dye removal at the optimum condition of 30.00 min, pH 4.32 and catalyst dose of 60 mg.

It can be seen that the catalytic properties of the prepared ZnS/TiO_2 nanocomposite is more similar to nano-sized TiO_2 rather than ZnS nanoparticles. The combination of ZnS and TiO_2 results in the improvement of photocatalyst performance for AB113 decolorization.

3.5. Kinetic modeling of the photodegradation process

The photodegradation kinetic models can be used as a tool for photoreactors design and scale-up (Hu et al., 2013). Fitting of the data to various models and their corresponding coefficients of determination (R^2) show that the kinetics of degradation of AB113 on the ZnS/TiO_2 nanoparticles can be explained more accurately by the pseudo second order and parabolic-diffusion models (Fig. 7). The R^2 is close to unity for these models.

The pseudo second order mechanism (PSOM) indicates that the rate limiting step is monolayer chemical sorption through photoinduced electron transfer between AB113 molecules and the ZnS/TiO_2 particles. The parabolic-diffusion model shows that electron transfer (the rate limiting step) is controlled by diffusion of the dye molecules from solution to the active sites of

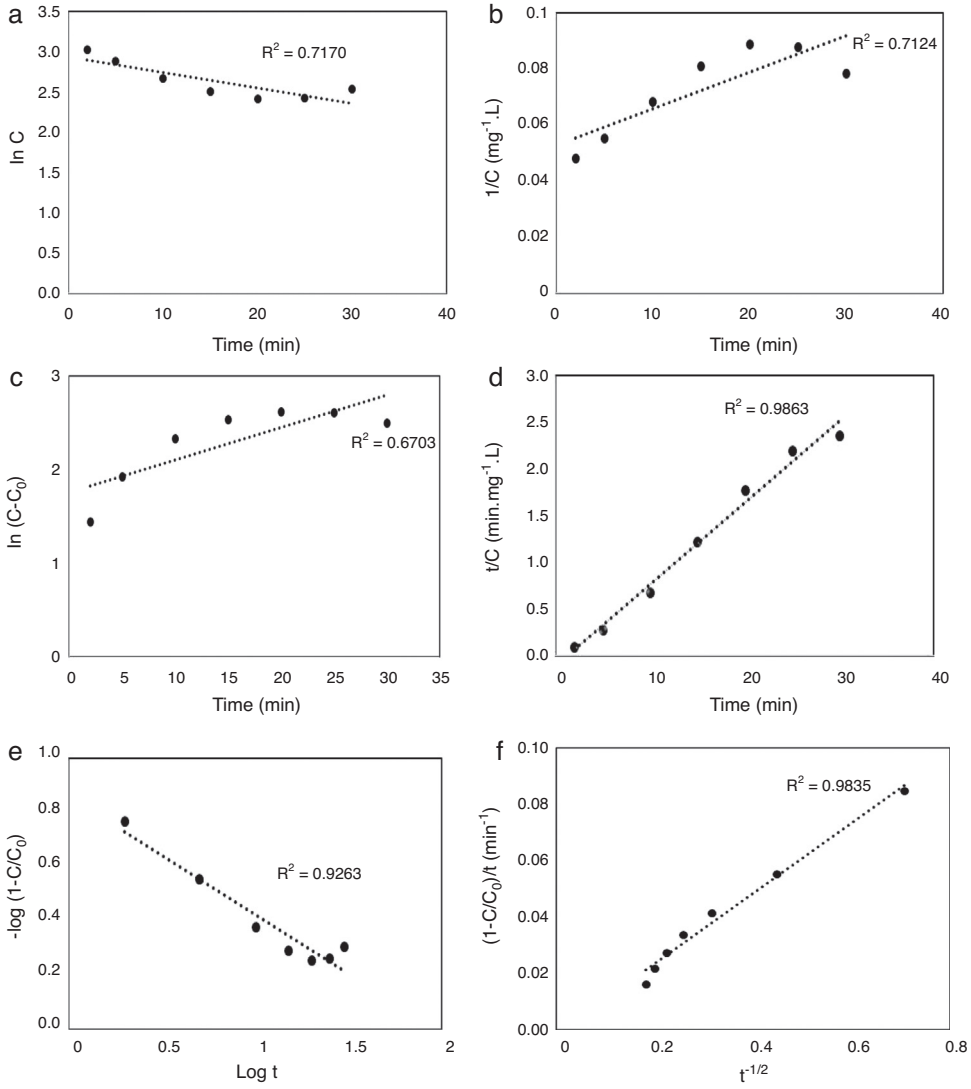

Fig. 7. Kinetic model of the photocatalytic degradation of AB113 on ZnS/TiO_2 nanoparticles (a) first-order, (b) second-order, (c) pseudo-first order, (d) pseudo-second-order, (e) modified Freundlich, and (f) parabolic diffusion models.

the catalyst (Hu et al., 2013). It can be concluded that the mechanism of dye removal by ZnS/TiO_2 includes diffusion, adsorption and photocatalytic degradation.

4. Conclusions

The nanoscale ZnS/TiO_2 hybrid photocatalyst was successfully synthesized using a chemical deposition method. The prepared composite was used for degradation of the azo dye Acid Blue 113 in the presence of UV-light. Response surface methodology with central composite rotatable design was effectively applied to the modeling and optimization of the process. Almost complete removal (99.0%) of the dye was achieved at the optimal conditions. The synthesized nanocomposite showed a higher photocatalytic activity than pure nano-sized TiO_2 and ZnS. The photodegradation of AB113 on the ZnS/TiO_2 nanoparticles obeyed the pseudo second order and parabolic-diffusion kinetic models. The obtained RSM and kinetic models can be used for further upscaling of the process.

Conflict of interest

The authors have no conflicts of interest to declare.

Acknowledgments

The authors would like to thank the support provided by the department of chemistry, University of Guilan.

References

Aisien, F. A., & Blessing, A. (2013). Photocatalytic degradation of 2, 2, 4 trimethyl pentane (isooctane) in aqueous solution. *Iranian Journal of Neonatology*, *4*(4), 1–7.

Bai, W., Cai, L., Wu, C., Xiao, X., Fan, X., Chen, K., & Lin, J. (2014). Alcohothermal synthesis of flower-like ZnS nano-microstructures with high visible light photocatalytic activity. *Materials Letters*, *124*, 177–180.

Beranek, R., & Kisch, H. (2008). Tuning the optical and photoelectrochemical properties of surface-modified TiO_2. *Photochemical & Photobiological Sciences*, *7*(1), 40–48.

Chaibakhsh, N., Ahmadi, N., & Zanjanchi, M. A. (2016). Optimization of photocatalytic degradation of neutral red dye using TiO_2 nanocatalyst via Box-Behnken design. *Desalination and Water Treatment*, *57*(20), 9296–9306.

De Moura, D. C., Quiroz, M. A., Da Silva, D. R., Salazar, R., & Martínez-Huitle, C. A. (2016). Electrochemical degradation of Acid Blue 113 dye using TiO_2-nanotubes decorated with PbO_2 as anode. *Environmental Nanotechnology, Monitoring & Management*, *5*, 13–20.

Dhatshanamurthi, P., Subash, B., Krishnakumar, B., & Shanthi, M. (2014). Highly active ZnS loaded TiO_2 photocatalyst for mineralization of phenol red sodium salt under UV-A light. *Indian Journal of Chemistry*, *53*(7), 820–823.

Dostanić, J., Lončarević, D., Rožić, L., Petrović, S., Mijin, D., & Jovanović, D. M. (2013). Photocatalytic degradation of azo pyridone dye: Optimization using response surface methodology. *Desalination and Water Treatment*, *51*(13–15), 2802–2812.

Franco, A., Neves, M., Carrott, M. R., Mendonça, M., Pereira, M., & Monteiro, O. (2009). Photocatalytic decolorization of methylene blue in the presence of TiO_2/ZnS nanocomposites. *Journal of Hazardous Materials*, *161*(1), 545–550.

Giwa, A., Nkeonye, P. O., Bello, K. A., & Kolawole, K. A. (2012). Photocatalytic decolourization and degradation of CI Basic Blue 41 using TiO_2 nanoparticles. *Journal of Environmental Protection*, *3*(9), 1063–1069.

Gosavi, V. D., & Sharma, S. (2014). A general review on various treatment methods for textile wastewater. *Journal of Environmental Science, Computer Science and Engineering & Technology*, *3*(1), 29–39.

Hu, A., Liang, R., Zhang, X., Kurdi, S., Luong, D., Huang, H., . . ., & Zhou, Y. (2013). Enhanced photocatalytic degradation of dyes by TiO_2 nanobelts with hierarchical structures. *Journal of Photochemistry and Photobiology A: Chemistry*, *256*, 7–15.

Jantawasu, P., Sreethawong, T., & Chavadej, S. (2009). Photocatalytic activity of nanocrystalline mesoporous-assembled TiO_2 photocatalyst for degradation of methyl orange monoazo dye in aqueous wastewater. *Chemical Engineering Journal*, *155*, 223–233.

Muhd Julkapli, N., Bagheri, S., & Bee Abd Hamid, S. (2014). Recent advances in heterogeneous photocatalytic decolorization of synthetic dyes. *The Scientific World Journal*, *2014*, 25. Article ID 692307.

Mukhlish, M. B., Najnin, F., Rahman, M. M., & Uddin, M. (2013). Photocatalytic degradation of different dyes using TiO_2 with high surface area: A kinetic study. *Journal of Scientific Research*, *5*(2), 301–314.

Myers, R. H., Montgomery, D. C., & Anderson-Cook, C. M. (2016). *Response surface methodology: Process and product optimization using designed experiments* (4th ed.). New Jersey: John Wiley & Sons.

Nachiyar, C. V., Sunkar, S., Kumar, G. N., Karunya, A., Ananth, P., Prakash, P., & Jabasingh, S. A. (2012). Biodegradation of acid blue 113 containing textile effluent by constructed aerobic bacterial consortia: Optimization and mechanism. *Journal of Bioremediation & Biodegradation*, *3*, 1–9.

Nageri, M., Kalarivalappil, V., Vijayan, B. K., & Kumar, V. (2016). Titania nanotube arrays surface-modified with ZnO for enhanced photocatalytic applications. *Materials Research Bulletin*, *77*, 35–40.

Pare, B., Swami, D., More, P., Qureshi, T., & Thapak, T. (2011). Mineralization of methylene violet dye using titanium dioxide in presence of visible light. *International Journal of Chemical Sciences*, *9*(4), 1685–1697.

Pouretedal, H., & Sohrabi, A. (2016). Photosensitization of TiO_2 by ZnS and bromo thymol blue and its application in photodegradation of para-nitrophenol. *Journal of the Iranian Chemical Society*, *13*(1), 73–79.

Roychowdhury, A., Pati, S. P., Kumar, S., & Das, D. (2014). Effects of magnetite nanoparticles on optical properties of zinc sulfide in fluorescent-magnetic Fe_3O_4/ZnS nanocomposites. *Powder Technology*, *254*, 583–590.

Sarici-Ozdemir, C. (2012). Adsorption and desorption kinetics behaviour of methylene blue onto activated carbon. *Physicochemical Problems of Mineral Processing*, *48*(2), 441–454.

Senapati, K. K., Borgohain, C., & Phukan, P. (2012). $CoFe_2O_4$–ZnS nanocomposite: A magnetically recyclable photocatalyst. *Catalysis Science & Technology*, *2*(11), 2361–2366.

Singh, K. P., Mohan, D., Sinha, S., Tondon, G., & Gosh, D. (2003). Color removal from wastewater using low-cost activated carbon derived from agricultural waste material. *Industrial & Engineering Chemistry Research*, *42*(9), 1965–1976.

Tian, X., Wen, J., Wang, S., Hu, J., Li, J., & Peng, H. (2016). Starch-assisted synthesis and optical properties of ZnS nanoparticles. *Materials Research Bulletin*, *77*, 279–283.

Tseng, H. H., Lee, W. W., Wei, M. C., Huang, B. S., Hsieh, M. C., & Cheng, P. Y. (2012). Synthesis of TiO_2/SBA-15 photocatalyst for the azo dye decolorization through the polyol method. *Chemical Engineering Journal*, *210*, 529–538.

Vaez, M., Zarringhalam Moghaddam, A., & Alijani, S. (2012). Optimization and modeling of photocatalytic degradation of azo dye using a response surface methodology (RSM) based on the central composite design with immobilized titania nanoparticles. *Industrial & Engineering Chemistry Research*, *51*(11), 4199–4207.

Wang, X., & Zhang, W. (2014). Chemical depositing of CdS/ZnS composition nanostructure modified TiO_2 thin film. *Chalcogenide Letters*, *11*(8), 389–395.

Wani, T. A., Ahmad, A., Zargar, S., Khalil, N. Y., & Darwish, I. A. (2012). Use of response surface methodology for development of new microwell-based spectrophotometric method for determination of atrovastatin calcium in tablets. *Chemistry Central Journal*, *6*(1), 134–142.

Xue, Z., Wang, T., Chen, B., Malkoske, T., Yu, S., & Tang, Y. (2015). Degradation of tetracycline with $BiFeO_3$ prepared by a simple hydrothermal method. *Materials*, *8*(9), 6360–6378.

Zanjanchi, M., Golmojdeh, H., & Arvand, M. (2009). Enhanced adsorptive and photocatalytic achievements in removal of methylene blue by incorporating tungstophosphoric acid–TiO_2 into MCM-41. *Journal of Hazardous Materials*, *169*(1–3), 233–239.